Fermion-induced dynamical critical point

Shuai Yin[1] and Shao-Kai Jian[2]
[1]*School of Physics, Sun Yat-Sen University, Guangzhou 510275, China*
[2]*Condensed Matter Theory Center, Department of Physics, University of Maryland, College Park, Maryland 20742, USA*

(Received 23 June 2020; revised 4 November 2020; accepted 24 February 2021; published 8 March 2021)

Dynamical phase transition (DPT) characterizes the abrupt change in dynamical properties in nonequilibrium quantum many-body systems. It has been demonstrated that extra fluctuating modes besides the conventional order parameter field can bring about the Landau-forbidden quantum critical points by changing the order of the equilibrium phase transition. However, the counterpart phenomena in DPTs have rarely been explored. Here, we study the DPT in the Dirac system after a sudden quench and find that the fermion fluctuations can round a putative first-order DPT into a dynamical critical point, which is referred to as a fermion-induced dynamical critical point (FIDCP). This FIDCP gives the universal short-time scaling behavior controlled by the dynamical chiral fixed point despite the system going through a first-order transition after thermalization. In the novel scenario of FIDCP, the quantum Yukawa coupling g_q is indispensable for inducing the FIDCP even though it is irrelevant in the infrared scale. We call these variables *dynamical dangerously irrelevant scaling variable*. Moreover, a dynamical tricritical point which separates the first-order DPT and the FIDCP is discovered by tuning this dynamical dangerously irrelevant scaling variable. We further mention possible experimental realizations.

DOI: 10.1103/PhysRevB.103.125116

I. INTRODUCTION

Fathoming nonequilibrium dynamics of isolated quantum systems is one of the most important and challenging issues in modern statistical mechanics and condensed-matter physics [1–3]. On the one hand, these studies provide fundamental insights into how equilibrium thermodynamics emerges from a unitary time evolution [4–8]. For example, the eigenstate thermalization hypothesis attempts to build the gorgeous edifice of the statistical ensemble theory upon the cornerstone of the eigenstate properties of quantum many-body systems [4–6]. On the other hand, emergences of vibrant far-from-equilibrium phenomena in experiments are calling for new theoretical frameworks [9–18]. Among them the theory of dynamical phase transition (DPT) has attracted considerable attention. By analogy with the equilibrium phase transition, the DPT describes the abrupt change in dynamical properties in nonequilibrium systems [19–43]. It has been shown that the appearance of the DPT can lead to universal short-time scaling behavior [44–48] similar to the critical initial slip in classical [49,50] and quantum dissipative systems [51–53].

In equilibrium phase transitions, the importance of fluctuations cannot be overemphasized. Long-wavelength fluctuations are at the origin of scaling behaviors near second-order phase transitions, which results in the concept of the universality class—one of the organizational principles in condensed-matter physics [54]. It is known that quantum fluctuations can strongly change the properties of equilibrium phases [55]. More strikingly, fluctuations can change the nature of the phase transition profoundly, giving phase transition beyond Landau's paradigm [56]. Coleman and Weinberg proposed a fluctuation-induced first-order phase transition by coupling the order parameter to a fluctuating gauge field [57–59]. This proposal found important applications in the context of phase transitions in the early universe and superconductors [58,59]. On the other hand, the theory of a deconfined quantum critical point [60–74] takes the opposite track by showing that extra fluctuations from emergent degrees of freedom can soften the putative first-order phase transition [56] into a continuous one. Another example is the fermion-induced quantum critical point (FIQCP) [75], in which the extra fluctuations come from massless Dirac fermions. It has been shown that both the Landau–de Gennes and Landau-Devonshire first-order phase transitions can be rounded into continuous ones by fermion fluctuations [76–82]. Given these novel examples in equilibrium physics, equally important questions in the context of nonequilibrium physics arise: To what extent is the DPT affected by extra fluctuations? Can the Landau-forbidden phase transition happen at nonequilibrium?

In this paper we report a fermion-induced dynamical critical point (FIDCP) in Dirac systems after a quench. We find that a putative nonequilibrium first-order DPT can be driven into a continuous one by fermion fluctuations, giving rise to a dynamical version of the Landau-forbidden critical point. We will show that this scenario of FIDCP gives plentiful intriguing phenomena in nonequilibrium relaxation process, as illustrated in Fig. 1. A counterintuitive result is that the universal dynamics appears only in the short-time stage controlled by the FIDCP, while it fades away in the long-time thermal stage. Moreover, we find that although the quantum Yukawa coupling is irrelevant near the renormalization group (RG) fixed point of the FIDCP, it plays an indispensable role

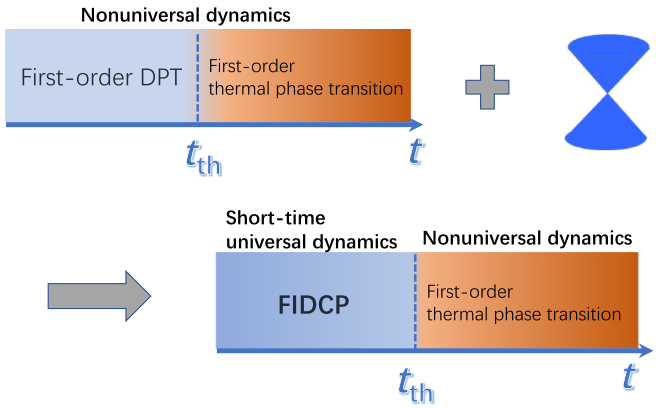

FIG. 1. An illustration of the fermion-induced dynamical critical point (FIDCP). The putative first-order dynamical phase transition can be induced to a dynamical critical point by gapless Dirac fermion fluctuations, leading to short-time universal dynamics before thermalization, although the discontinuous thermal transition survives in the long-time thermal stage.

in bringing out the FIDCP, in contrast to usual irrelevant scaling variables which are negligible in equilibrium phase transitions. We refer to this kind of scaling variable as the *dynamical* dangerously irrelevant scaling variable (DISV), reminiscent of the DISV in equilibrium Landau-forbidden phase transitions [61,70,79,80]. In spite of this, we will show that the dynamical DISV in the FIDCP is quite different from the equilibrium DISV in the equilibrium Landau-forbidden critical points [70,79,80]. It is "more dangerous" since its ultraviolet (UV) value can manipulate a dynamical tricritical point (DTCP), which is the watershed between the first-order DPT and the FIDCP. We will show that this DTCP corresponds to a nonthermal fixed point, which cannot be cast to any thermal/quantum critical point. Some sharp physical consequences and a lattice model, which should be within the experimental reach, will also be discussed.

This paper is organized as follows. In Sec. II we show the model and the quench protocol. Then in Sec. III the FIDCP is illuminated. We first present the RG equations in Sec. III A. Then we show in Sec. III B that a first-order DPT appears without the Yukawa coupling. In Sec. III C we demonstrate that this first-order DPT can be rounded to a dynamical critical point by large enough Yukawa coupling. In Sec. IV, the critical properties near the DTCP are further explored. Possible experimental realization is then discussed in Sec. V. We conclude with a brief summary in Sec. VI. Some supplementary results and a lattice model are briefly discussed in the Appendixes.

II. MODEL AND QUENCH PROTOCOL

We consider the quench dynamics in a system with a negative quartic boson interaction and study the effects induced by its coupling with Dirac fermions. The nonequilibrium dynamics is described by the generating function $Z = \mathrm{Tr}[e^{iS_K}]$ [44–47]. The Keldysh action $S_K \equiv iS_i + S_b$ therein consists of two parts, S_i and S_b, corresponding, respectively, to the initial state and the postquench dynamics, where [48]

$$\begin{aligned} S_i &= \frac{1}{2}\int_x \int_0^\infty d\tau[(\partial_\tau\phi)^2 + (\nabla\phi)^2 + \Omega^2\phi^2], \\ S_b &= \int_x \int_0^\infty dt\Big[(\dot{\phi}_q\dot{\phi}_c - \nabla\phi_c\nabla\phi_q - r\phi_c\phi_q) \\ &\quad - \frac{2u_c}{4!}\phi_c^3\phi_q - \frac{2u_q}{4!}\phi_q^3\phi_c + \Psi^\dagger(i\partial_t + i\vec{\sigma}\cdot\nabla)\Psi \\ &\quad - \frac{g_c}{\sqrt{2}}\phi_c\Psi^\dagger\sigma_z\Psi - \frac{g_q}{\sqrt{2}}\phi_q\Psi^\dagger\tau_x\sigma_z\Psi + \cdots\Big], \end{aligned} \tag{1}$$

in which the subscripts c and q represent the classical and quantum parts of the action, respectively, in the Keldysh representation. ϕ is the Ising boson field, and $\Psi \equiv (\psi_c, \psi_q)^T$ is the Dirac fermion field. The summation over N flavors is assumed. $\int_x \equiv \int d^dx$, where d is the spatial dimension, $\vec{\sigma} \equiv (\sigma_x, \sigma_y)$ is the Dirac matrix in two dimensions and can be generalized accordingly to higher dimensions, and τ_x acts on the Keldysh contour. $u_{c/q} < 0$ is the boson quartic coupling, $g_{c/q} > 0$ is the Yukawa coupling, and the ellipses represent the higher-order terms to stabilize the system (see Appendix D). The system is initially prepared in the disordered phase with a boson mass $\Omega^2 > 0$; then at $t = 0$ the boson mass is suddenly changed r, and the system evolves according to the postquench Hamiltonian.

For $\Omega^2 = r$, Eq. (1) with $u_{c/q} < 0$ returns to the equilibrium case describing the equilibrium type-II FIQCP. It was shown that although at zero temperature a bosonic first-order phase transition [83] can be rounded by fermion fluctuations [82], the first-order phase transition can reappear at finite temperatures since the massless fermion fluctuation is inhibited by the finite Matsubara frequency gap proportional to the temperature [82]. So this argument indicates that the dynamical version of the FIQCP may not occur since the injection of the external energy by the sudden quench for $\Omega^2 \neq r$ is similar to the thermal effects according to the eigenstate thermalization hypothesis [4–6]. Surprisingly, we will show that the FIDCP can happen at the short-time stage in the following.

We will focus on the deep quench for $\Omega \gg \Lambda$, with Λ^2 being the UV momentum scale [44–47,84]. In this situation, the DPT is tuned by the renormalized boson mass,

$$\begin{aligned} r_{\mathrm{eff}}(t) &= r + \frac{1}{2}\int d^dk D_K(t,t) \\ &\quad - \frac{g_c g_q}{2}\int_0^t dt' \int d^dk \mathrm{Tr}[\tau_0\sigma_z G(t,t')\tau_x\sigma_z G(t',t)], \end{aligned} \tag{2}$$

in which $D_K(t,t') \equiv -i\langle\phi_c(t)\phi_c(t')\rangle$ is the boson Keldysh Green's function and $G(t,t') \equiv -i\langle\Psi(t)\Psi^\dagger(t')\rangle$ is the fermion Green's function. For the deep quench, $D_K(t,t') \simeq -i\Omega[\cos\omega_k(t-t') - \cos\omega_k(t+t')]/\omega_k^2$ [44–47], $\omega_k^2 \equiv \vec{k}^2 + r$. Note that the initial condition is contained in $D_K(t,t')$ and the second term in $D_K(t,t')$ breaks the time-translational symmetry explicitly. By comparing $D_K(t,t')$ with the thermal Keldysh function, $D_K^{(\mathrm{th})}(t,t') \simeq 2T\cos\omega_k(t-t')/\omega_k^2$, one finds that Ω is similar to an effective temperature $T_{\mathrm{eff}} = \Omega/4$ [44–47]. Although r_{eff} oscillates with a frequency proportional to Λ, the universal behavior of the DPT is contained

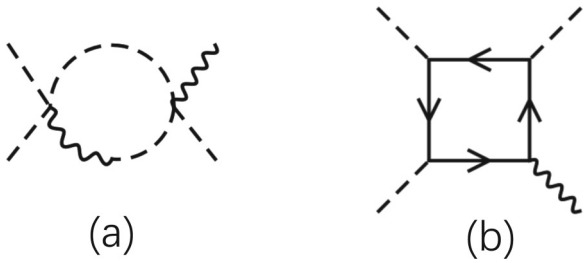

FIG. 2. The Feynman diagrams for the one-loop corrections to u_c. The dashed line presents the classical boson field, the wiggly line presents the quantum bosonic field, and the solid line indicates the fermion field.

in its time-independent part. The DPT controlled by Eq. (2) happens in a short-time stage before the thermalization time $t_{\rm th}$ [44–47]. After $t_{\rm th}$, the secular terms with dissipation effects dominate, and the system tends to the thermal state [85,86].

III. FERMION-INDUCED DYNAMICAL CRITICAL POINT

A. RG equations

To explore the DPT properties, we resort to the RG analyses. By integrating out the momentum within the range $[\Lambda, \Lambda e^{-l}]$ ($l > 0$ is the running parameter) for the inner line of the Feynman diagrams (some Feynman diagrams are shown in Fig. 2 for illustration) and rescaling the couplings according to $k \to ke^{l}$, $u_c \to u_c e^{l(4-d-2\eta_b)}$, $u_c \to u_c e^{l(2-d-2\eta_b)}$, $g_c^2 \to g_c^2 e^{l(4-d-\eta_b-2\eta_f)}$, and $g_q^2 \to g_q^2 e^{l(2-d-\eta_b-2\eta_f)}$, one obtains the following RG equations [48]:

$$\frac{du_c}{dl} = (4-d-2\eta_b)u_c - \frac{3}{8}u_c^2 + 6Ng_c^3 g_q, \tag{3}$$

$$\frac{du_q}{dl} = (2-d-2\eta_b)u_c - \frac{3}{8}u_c u_q + 6Ng_c g_q^3, \tag{4}$$

$$\frac{dg_c^2}{dl} = (4-d-\eta_b-2\eta_f)g_c^2 - \frac{3}{8}g_c^4 - \frac{3}{8}g_c^3 g_q, \tag{5}$$

$$\frac{dg_q^2}{dl} = (2-d-\eta_b-2\eta_f)g_q^2 - \frac{3}{8}g_c^2 g_q^2 - \frac{3}{8}g_c g_q^3, \tag{6}$$

where N is the flavor number of the Dirac fermions and $\eta_b = Ng_c g_q/4$ and $\eta_f = g_c^2/12 + g_c g_q/12$ are the anomalous dimensions of the boson and fermion fields, respectively. The boson mass r is relevant as a transition-tuning parameter, so we set r to zero in Eqs. (3)–(6) to describe scaling properties. Although in the UV scale $u_c = u_q$ and $g_c = g_q$, the classical part and the quantum part of the couplings have different dimensions for the deep quench case since Ω is dimensionless, similar to the status of the temperature in classical phase transitions [44–47]. And we will see that the quantum Yukawa coupling plays a vital role in the FIDCP.

B. First-order DPT without Yukawa coupling

When $g_{c/q} = 0$ and $u_{c/q} < 0$ at the UV scale, Eqs. (3) and (4) show that in the infrared (IR) scale u_c tends to negative infinity. It is quite different from the case for $u_c > 0$, where a finite IR fixed point is reached [44–47]. Actually, Eq. (3) is similar to the RG flow equation of the quartic boson coupling in the equilibrium d-dimensional Landau-Devonshire model [83], indicating that the DPT is a first-order DPT [83]. This similarity also exists between the $(d+1)$-dimensional dynamical fixed point and the d-dimensional Wilson-Fisher fixed point for the pure boson model [44–47]. The absence of the finite IR fixed point demonstrates that there is no self-similarity aging dynamics near this first-order DPT.

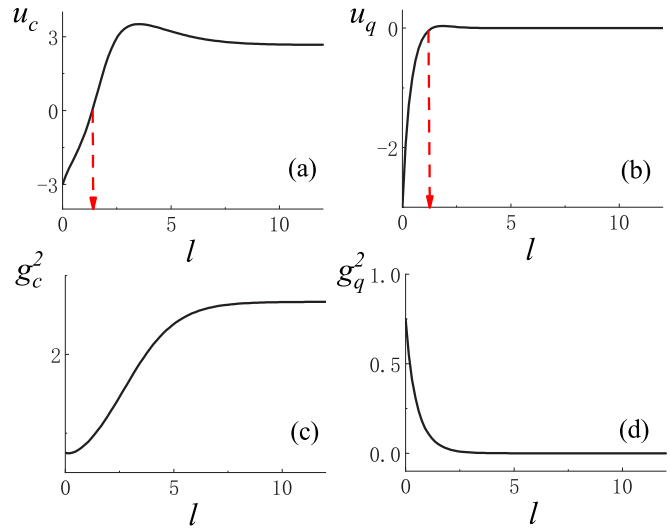

FIG. 3. For $N = 2$ and $d = 3$, the RG flows running from $l = 0$ (UV) to $l \to \infty$ (IR) are shown. The bare parameters are chosen to be $u_c(0) = u_q(0) = -3$ and $g_c^2(0) = g_q^2(0) = 0.75$. (a) shows that u_c runs from a negative value to a positive one. (b) shows u_q also changes sign and then tends to zero. The arrows in (a) and (b) denote positions of the sign changes for u_c and u_q, respectively. g_c tends to a finite fixed point, as shown in (c), and g_q tends to zero, as shown in (d).

C. FIDCP with Yukawa coupling

Remarkably, the situation can be changed when the coupling to the Dirac fermion is introduced. We will show that the gapless fluctuations of the Dirac fermion can trigger an emergent dynamical critical point, and as a result the universal dynamics governed by the long-wavelength modes near this FIDCP appears. To see this, one can inspect Eq. (3). The anticommutativity of the fermion fields leads to an additional minus sign in the fermionic loop diagram, as shown in Fig. 2(b). This makes the last term in Eq. (3) positive. Accordingly, the last term makes an opposite contribution compared to the first two terms. Heuristically, the direction of the RG flow of u_c can be changed for large enough $g_{c/q}$.

To quantitatively explore the FIDCP, we solve the RG equations (3)–(6) explicitly by taking $N = 2$ and $d = 3$ as an example and show the results in Fig. 3. From Fig. 3(a) one finds that for a finite UV $g_{c/q}$, u_c changes sign from negative to positive and then tends to an IR fixed point. Moreover, the massless boson correlation can induce a nontrivial Yukawa fixed point, as shown in Fig. 3(c), via the one-loop correction to the Yukawa coupling. The appearance of the finite fixed point demonstrates that the fermion fluctuation can induce a dynamical critical point.

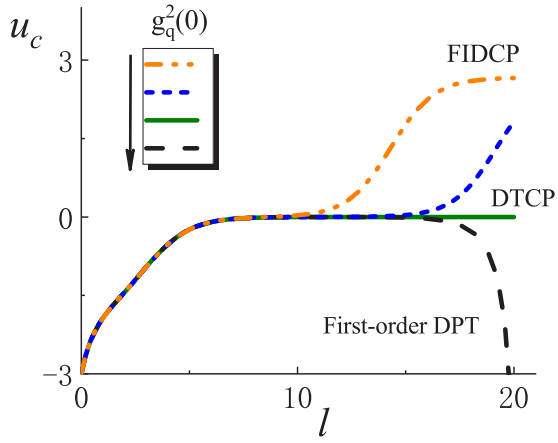

FIG. 4. For $N = 2$ and $d = 3$, a fixed point corresponding to a DTCP is determined by tuning g_q. Other parameters in the UV scale are chosen to be $u_c(0) = u_q(0) = -3$ and $g_c^2(0) = g_q^2(0)$. At the DTCP, $g_{q\mathrm{tr}}^2(0) \simeq 0.726624313854$. u_c is relevant at the DTCP, and its fixed-point value is zero. g_c tends to a finite value, indicating this is a nonthermal fixed point. Both u_q and g_q are irrelevant in the IR limit.

The critical behavior associated with the FIDCP is determined by the properties of the fixed point. Actually, the fixed point of the FIDCP is just the dynamical chiral fixed point reported previously [48]. This fixed point is a nonthermal with a nonzero value of the g_c since it should be zero in the thermal critical point owing to the finite Matsubara frequency gap. The most remarkable phenomenon associated with this fixed point is the universal critical initial slip behavior, in which the boson order parameter M changes with time as $M \propto M_0 t^\theta$, with θ being the critical initial slip exponent [44–48]. Moreover, the fermion field has an anomalous dimension $\eta_f = (4-d)/12$ [48].

Although the FIDCP with $u_{c/q}(0) < 0$ has the same dynamical universality class as the case for $u_{c/q}(0) > 0$, the quantum part of the Yukawa coupling g_q plays different roles in these two cases. For the latter case, g_q is just a usual irrelevant scaling variable which is negligible near the phase transitions. But for the former case, the role played by g_q is quite nontrivial, although it also tends to zero near the dynamical chiral Ising fixed point. To see this, by setting g_q to zero in the UV scale [87], one finds from Eq. (3) that the fermion fluctuations do not participate in the postquench dynamics, resulting in a first-order DPT, as we discussed above. It is the finite g_q, together with g_c, at the UV scale that brings fermion fluctuations into the boson potential, reverses the sign of $u_{c/q}$, and, consequently, results in the dynamical chiral Ising fixed point and generates the universal critical initial slip behavior. In this sense, we find that g_q is a dynamical DISV.

IV. DYNAMICAL TRICRITICAL POINT

In the equilibrium case, appearances of dangerously irrelevant scaling variables can reshape critical properties in both the deconfined quantum critical point and the FIQCP [70,79,80]. Here we show in Fig. 4 that the dynamical dangerously irrelevant scaling variable g_q plays a different role and can maneuver a DTCP, although it is still irrelevant near this DTCP. This DTCP appears at $g_{q\mathrm{tr}}(0)$ when other parameters are fixed at the UV scale. And only for $g_q(0) > g_{q\mathrm{tr}}(0)$ can the FIDCP arise. At the fixed point of this DTCP, $u_{c\mathrm{tr}}^* = 0$. Besides r, whose scaling is relevant, $r \propto re^{2l}$, Fig. 4 shows that u_c is the other relevant direction near the DTCP. When $g_q(0)$ is close to $g_{q\mathrm{tr}}(0)$, u_c lingers over a plateau for a period of scale, then tends to negative infinity or the dynamical chiral fixed point depending on whether $g_q(0) < g_{q\mathrm{tr}}(0)$ or $g_q(0) > g_{q\mathrm{tr}}(0)$. From Eq. (3) one finds that u_c deviates from $u_{c\mathrm{tr}}^*$ by $u_c \propto u_c e^l$.

Some remarks on the DTCP are as follows: (a) An intriguing feature of the DTCP is that although g_q is an irrelevant variable near the DTCP, it can control the direction of the relevant variable u_c. This cross-rank tuning behavior has rarely been reported in the usual equilibrium phase transitions, including the type-II FIQCP. (b) g_c tends to a finite value at DTCP, indicating that this fixed point is a nonthermal fixed point. (c) The larger the fermion flavor number N is, the smaller $g_{q\mathrm{tr}}(0)$ becomes since more fermion fluctuations can be taken into account according to Eq. (3). (d) The DTCP appears only for $u_{c/q} < 0$, while for $u_{c/q} > 0$ the short-time dynamical phase transition is always a continuous one with critical phenomena controlled by the dynamical chiral fixed point [48].

V. DISCUSSION

The results obtained above provide several sharp experimental signatures. To see this, we compare different cases. (a) When $u > 0$, the universal behaviors exist in both the short-time stage and the thermalization stage [48]. According to the eigenstate thermalization hypothesis, the scaling behavior in the thermalization stage is just the classical phase transition governed by the Wilson-Fisher fixed point [88–90]. (b) When $u < 0$ and $g < g_{\mathrm{tr}}$ is small, the quench dynamics does not show any universal scaling behavior in any stage after the quench since both the DPT and the thermal phase transition are first order. (c) When $u < 0$ and $g > g_{\mathrm{tr}}$ is large enough to bring out the FIDCP, universal scaling behaviors emerge in the short-time relaxation stage. After the equilibration $t \gg t_{\mathrm{th}}$ in the thermal region, the Matsubara frequency of fermion modes opens a gap proportional to the effective temperature $T_{\mathrm{eff}} \gg \Lambda^2$. Thus, the mechanism of the FIDCP is interdicted, and consequently, the long-time thermal region exhibits no universal scaling properties.

Here, we propose a possible experimental realization. It was shown that the spin model with the nearest and next-nearest Ising interactions can host a first-order phase transition described by the boson field theory with a negative quartic interaction, i.e., $u < 0$ [91]. In addition, the Dirac systems can be realized in the honeycomb lattice and the square lattice with π-flux per plaquette [92,93]. Recently, steerable magnetic interactions were implemented experimentally in various cold-atom systems [94,95]. Moreover, manipulation and detection of nonequilibrium dynamics have been realized in plenty of systems [96,97]. In particular, short-time scaling behaviors were found in recent experiments [98–100]. It is expected that the FIDCP could be realized in these systems with tunable interaction between bosons and Dirac fermions. Based on the model in Ref. [91], we briefly discuss possible parameter regions to realize the FIDCP in Appendix E.

VI. SUMMARY AND OUTLOOK

We have studied dynamical phase transitions in Dirac systems and reported an FIDCP. We have shown that a first-order DPT for the pure boson model can be rounded by the fermion fluctuations into a dynamical critical point, corresponding to the dynamical chiral Ising fixed point in our case. In the scenario of FIDCP, the quantum Yukawa coupling is a dynamical DISV, which plays a crucial role in inducing the FIDCP even though it is irrelevant near the critical point. The existence of dynamical DISV makes the notion of continuous/discontinuous transitions in dynamical phase transitions different from that in equilibrium ones. Furthermore, a DTCP associated with the dynamical DISV was identified, and its scaling properties were discussed.

Our paper not only shows that the Landau-forbidden critical point can happen in nonequilibrium but also provides experimental criteria to detect it. Our results can be generalized to Dirac/Weyl systems with different boson fields [101]. Moreover, it is instructive to explore the nonequilibrium dynamics in itinerant electronic systems with finite Fermi surfaces, in which the tendency to turn the first-order transition into a continuous one was found in equilibrium cases [102,103].

ACKNOWLEDGMENTS

We wish to thank F. Zhong and G.-Y. Huang for their helpful discussions. S.Y. is supported by the Natural Science Foundation of China (Grant No. 41030090). S.-K.J. is supported by the Simons Foundation through the It from Qubit Collaboration.

S.-K.J. and S.Y. contributed equally to this work.

APPENDIX A: THE GREEN'S FUNCTIONS

To obtain the RG equations, the Gaussian Green's functions for both fermion and boson fields are needed. For a general initial boson mass Ω, the Green's functions for the free-boson fields read [44–48]

$$D_R(t-t') = -\Theta(t-t')\frac{\sin\omega_k(t-t')}{\omega_k}, \tag{A1}$$

$$D_K(t,t') = -i\frac{1}{\omega_k}[K_+\cos\omega_k(t-t') + K_-\cos\omega_k(t+t')], \tag{A2}$$

in which D_R is the retarded Green's function, D_K is the Keldysh Green's function $\omega_k = \sqrt{k^2+r}$, and $K_\pm = \frac{1}{2}[\frac{\omega_k}{\omega_{0k}} \pm \frac{\omega_{0k}}{\omega_k}]$, with ω_{0k} being $\omega_{0k} = \sqrt{k^2+\Omega}$. In the deep quench limit, in which $\Omega \gg \Lambda^2$, Eq. (A2) can be simplified as

$$D_K(t,t') = -i\frac{\Omega}{\omega_k^2}[\cos\omega_k(t-t') - \cos\omega_k(t+t')]. \tag{A3}$$

In addition, the Green's functions for the fermion fields are [48]

$$G_R(t-t') = -i\Theta(t-t')[e^{-ik(t-t')}P_+(k) + e^{ik(t-t')}P_-(k)], \tag{A4}$$

$$G_K(t,t') = -i[e^{-ik(t-t')}P_+(k) - e^{ik(t-t')}P_-(k)], \tag{A5}$$

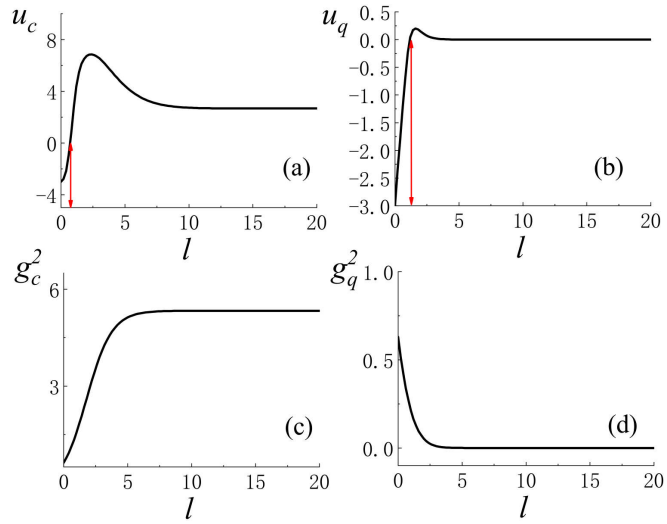

FIG. 5. For $N = 2$ and $d = 2$, the RG flows running from $l = 0$ (UV) to $l \to \infty$ (IR) are shown. The bare parameters are chosen to be $u_c(0) = u_q(0) = -3$ and $g_c^2(0) = g_q^2(0) = 0.7$. (a) shows that u_c runs from a negative value to a positive one. (b) shows u_q also changes sign and then tends to zero. The arrows in (a) and (b) denote positions of the sign changing for u_c and u_q, respectively. g_c tends to a finite fixed point, as shown in (c), and g_q tends to zero, as shown in (d).

in which $k = \sqrt{k_x^2+k_y^2}$ and $P_\pm = \frac{1}{2}(1 \pm \hat{k}\cdot\vec{\sigma})$, with $\hat{k} = (k_x, k_y)/k$. Equations (A4) and (A5) can be readily generalized to higher dimensions by taking more momentum components into account.

APPENDIX B: FIDCP in $d = 2$

Here, we show the FIDCP in $d = 2$. By solving the RG equations (3)–(6), we show that in two dimensions the fermion fluctuations can also round the first-order DPT into a dynamical critical point, similar to the case for $d = 3$. The results are plotted in Fig. 5. In Fig. 5, $u_{c/q}(0)$ are chosen to be identical to those in Fig. 3 in the main text, but $g_{c/q}^2(0)$ is smaller than that for $d = 3$. This indicates that in two dimensions, the effects induced by the fermion fluctuations are more apparent.

In addition, the DTCP for $d = 2$, which is realized by tuning g_q, is also found, as shown in Fig. 6. For the same other parameters, $g_{g\text{tr}}$ is smaller than its counterpart in $d = 3$.

APPENDIX C: TRICRITICAL POINT FOR DIFFERENT N

Here, we study the dependence of $g_{q\text{tr}}(0)$ on N. We take the case for $d = 3$ as an example. Figure 7 shows the results. From Fig. 7 one finds that the tricritical point $g_{q\text{tr}}^4(0)$ decrease as N increases. By power fitting, one finds that $g_{q\text{tr}}(0)$ satisfies $g_{q\text{tr}}^4(0) \propto 1/N$ approximatively. To determine the reason, one can estimate the value of $g_{q\text{tr}}(0)$ by inspecting Eq. (3), from which one finds the right-hand side of Eq. (3) changes sign when

$$g^4(0) > \frac{3u_c(0)[6u_c(0) - 8(4-d)]}{48N}. \tag{C1}$$

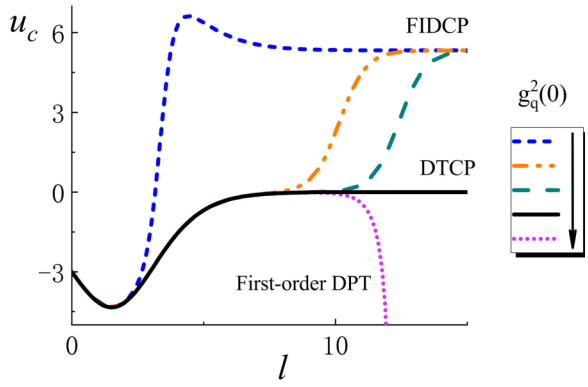

FIG. 6. For $N = 2$ and $d = 2$, a fixed point corresponding to a DTCP is determined by tuning g_q. Other parameters in the UV scale are chosen to be $u_c(0) = u_q(0) = -3$ and $g_c^2(0) = g_q^2(0)$. At the DTCP, $g_{q\mathrm{tr}}^2(0) \simeq 0.6991382539535241$. u_c is relevant at the DTCP, and its fixed-point value is zero. g_c tends to a finite value, indicating this is a nonthermal fixed point. Both u_q and g_q are irrelevant in the IR limit.

However, in this approximation, the contributions from the anomalous dimension have been neglected. This may also be the reason for the deviation from $1/N$, as shown in Fig. 7.

APPENDIX D: FIDCP WITH HIGHER-ORDER BOSON COUPLING

In the main text, we keep the terms which make leading contributions in the UV and IR scales near the transition point. When $u < 0$, at least one positive higher-order boson coupling is needed to stabilize the system. In this section, we show that our main results are not altered by the higher-order boson couplings. Concretely, we assume that the sixth-order boson coupling is positive and higher-order terms are neglected. By casting this term into the closed time path integral, one obtains an additional term, $\int_0^\infty dt \int d^dx[-\frac{v_c}{6!}\frac{3}{2}\phi_c^5\phi_q - \frac{v_q}{6!}\frac{3}{2}\phi_q^5\phi_c - \frac{v_i}{6!}5\phi_q^3\phi_c^3]$, in Eq. (1). Physically, the coupling $v(0)$

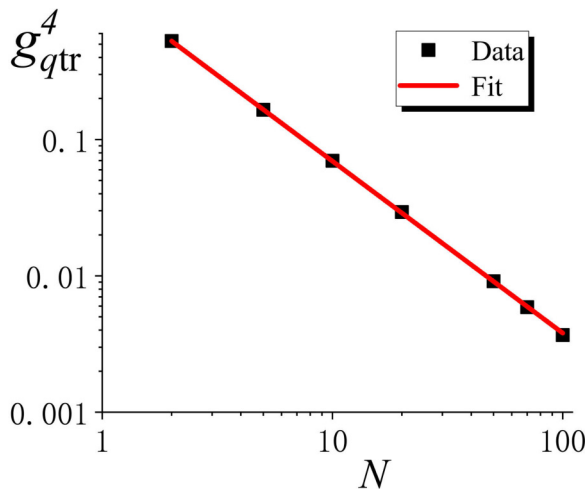

FIG. 7. Curves of the tricritical point g_{tr}^4 versus N. The boson quartic coupling is chosen to be $u(0) = -3$. Double logarithmic scales are used. Power fitting shows that $g_{\mathrm{tr}}^4 \propto 1/N_f^{1.12}$.

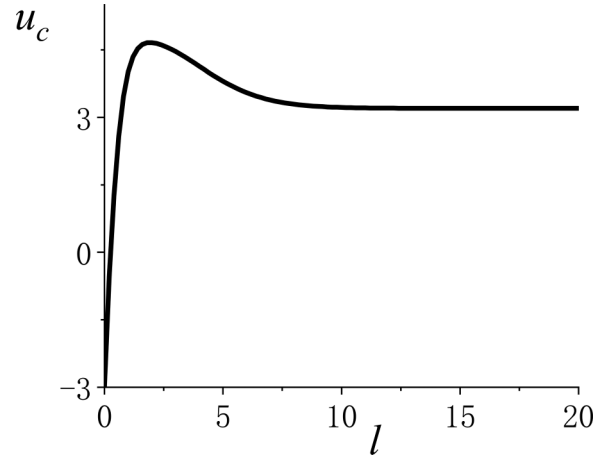

FIG. 8. For $N = 2$ and $d = 3$, the RG flow for u_c running from $l = 0$ (UV) to $l \to \infty$ (IR). The bare parameters are chosen to be $u_c(0) = -3$, $v_c(0) = 0.1$ and $g_c^2(0) = g_q^2(0) = 1.2$. u_c changes sign and tends to the dynamical chiral Ising fixed point in the IR scale. For $g_{c/q}^2(0) < g_{c/q\mathrm{tr}}^2(0) \simeq 0.9$, u_c tends to negative infinity.

should be far smaller than $|u(0)|$ and $g(0)$ because it describes three-body collision processes. In the deep quench case, v_q scales as $v_q \sim v_q(0)e^{l(2-2d-3\eta_b)}$, and v_i scales as $v_i \sim v_i(0)e^{l(4-2d-3\eta_b)}$. Both of them are less relevant than u_q and play ignorable roles. We then obtain the one-loop RG equations by taking into account the contribution from v_c as

$$\frac{du_c}{dl} = (4-d-2\eta_b)u_c - \frac{3}{8}u_c^2 + 6Ng_c^3g_q + \frac{1}{8}v_c, \quad \text{(D1)}$$

$$\frac{dv_c}{dl} = (6-2d-3\eta_b)u_c + \frac{15}{8}u_c^3 - \frac{15}{4}u_cv_c + \frac{345}{4}Ng_c^5g_q, \quad \text{(D2)}$$

$$\frac{dg_c^2}{dl} = (4-d-\eta_b-2\eta_f)g_c^2 - \frac{3}{8}g_c^4 - \frac{3}{8}g_c^3g_q, \quad \text{(D3)}$$

$$\frac{dg_q^2}{dl} = (2-d-\eta_b-2\eta_f)g_q^2 - \frac{3}{8}g_c^2g_q^2 - \frac{3}{8}g_cg_q^3. \quad \text{(D4)}$$

By solving Eqs. (D2)–(D4), one finds two nontrivial fixed points. One is $(u_c, g_c^2, v_c) = (\frac{8\varepsilon}{3}, \frac{8\varepsilon}{3}, O(\varepsilon^2))$. This is the dynamical chiral Ising fixed point [48]. The other is $(u_c, g_c^2, v_c) = (-\frac{16}{25} + \frac{88\varepsilon}{75}, \frac{8\varepsilon}{3}, \frac{768+384\varepsilon}{625})$. This is the dynamical tricritical point with u_c being its second relevant direction, as we discussed in the main text. In Fig. 8, we show that the FIDCP can arise even with a finite $v_c(0)$.

APPENDIX E: POSSIBLE EXPERIMENTAL REALIZATION

It has been demonstrated that the first-order phase transition with negative quartic coupling can be realized with the following spin Hamiltonian in the square lattice [91]:

$$H_s = J_1\sum_{\langle i,j\rangle} s_i^z s_j^z - J_2\sum_{\langle\langle i,j\rangle\rangle} s_i^z s_j^z - h_z\sum_i s_i^z - \Gamma\sum_i s_i^x, \quad \text{(E1)}$$

in which $s^{x/z}$ is the Pauli matrix, $J_1 > 0$, $J_2 < 0$, $\langle\cdot\rangle$ and $\langle\langle\cdot\rangle\rangle$ represent the nearest and next-nearest couplings, respectively, h_z is the longitudinal field, and Γ is the transverse field. The expectation value of s^z, i.e.,

$\langle s^z \rangle$, can be decomposed into the ferromagnetic part and the antiferromagnetic part. For the A sublattice, $\langle s^z \rangle = m_f + \phi$, while for the B sublattice, $\langle s^z \rangle = m_f - \phi$. For $J_1 = J_2$, the ferromagnetic order parameter m_f is just a background field. Accordingly, the low-energy effective theory for this model can be described by its antiferromagnetic order parameter ϕ, whose free energy reads

$$f = f_0 + \frac{r}{2}\phi^2 + \frac{u}{4!}\phi^4 + \cdots, \tag{E2}$$

in which ϕ is the antiferromagnetic order parameter, f_0 is independent of ϕ, $r = 2(J_1 + J_2)[1 - \frac{4\Gamma^2(J_1+J_2)}{(h_z^2+\Gamma^2)^{3/2}})]$, and $u = \frac{24(\Gamma^2-4h_z^2)\Gamma^2(J_1+J_2)^4}{8(h_z^2+\Gamma^2)^{7/2}}$. Accordingly, for $u < 0$, i.e., $\Gamma < 2h_z$, model (E2) hosts an equilibrium Landau-Devonshire first-order phase transition by tuning r [83]. Moreover, as we discussed in the main text, this model also exhibits first-order dynamical phase transition after a sudden quench.

In addition, a square lattice with the π flux per plaquette hosts a gapless Dirac fermion with the Hamiltonian as follows [92]:

$$H_f = i\bar{\psi}\gamma \cdot \nabla\psi, \tag{E3}$$

in which γ is the gamma matrices, $\bar{\psi} = \psi^\dagger\gamma^0$, and the summation over the flavors of ψ is implicit.

Then, the coupling between models (E2) and (E3) is the usual Yukawa coupling,

$$H_{co} = g\phi\bar{\psi}\psi. \tag{E4}$$

The effective action describing the quench dynamics of the lattice model (E2)–(E4) is just Eq. (1) in the main text. So the FIDCP described in the main text could be realized in the quench dynamics of these systems by tuning the coupling strength.

In addition, one can also consider model (E1) in the honeycomb lattice. In this case, $r = 3(J_1 + 2J_2)[1 - \frac{9\Gamma^2(J_1+2J_2)}{(h_z^2+\Gamma^2)^{3/2}})]$, and $u = \frac{81(\Gamma^2-4h_z^2)\Gamma^2(J_1+2J_2)^4}{4(h_z^2+\Gamma^2)^{7/2}}$. Also, for $\Gamma < 2h_z$, $u < 0$, and the system features a dynamical first-order phase transition, as we discussed in the main text. Moreover, it is well known that the band structure in the honeycomb lattice exhibits Dirac points [93]. When the fermion surface is at the Dirac points, the effective Hamiltonian is Eq. (E3).

It has been demonstrated that many magnetic phases and their dynamics have been realized in various kinds of lattice systems, including the honeycomb lattice, with ultracold fermions [94]. Thus, the FIDCP reported in the main text may also be detected in these systems. In particular, as we discussed in the main text, for small g, the dynamical phase transition in the short-time region should be first order, and the equilibrium phase transition after thermalization should also be first order; however, for large g, the dynamical phase transition in the short-time region should be continuous, giving the critical initial slip behavior [48], and the equilibrium phase transition after thermalization is still first order. This difference can provide sharp signatures to detect the FIDCP in experiments.

[1] J. Dziarmaga, Adv. Phys. **59**, 1063 (2010).
[2] A. Polkovnikov, K. Sengupta, A. Silva, and M. Vengalattore, Rev. Mod. Phys. **83**, 863 (2011).
[3] L. D'Alessio, Y. Kafri, A. Polkovnikov, and M. Rigol, Adv. Phys. **65**, 239 (2016).
[4] J. M. Deutsch, Phys. Rev. A **43**, 2046 (1991).
[5] M. Srednicki, Phys. Rev. E **50**, 888 (1994).
[6] M. Rigol, V. Dunjko, and M. Olshanii, Nature (London) **452**, 854 (2008).
[7] C. Neill *et al.*, Nat. Phys. **12**, 1037 (2016).
[8] A. Polkovnikov and D. Sels, Science **353**, 752 (2016).
[9] M. Gring, M. Kuhnert, T. Langen, T. Kitagawa, B. Rauer, M. Schreitl, I. Mazets, D. A. Smith, E. Demler, and J. Schmiedmayer, Science **337**, 1318 (2012).
[10] T. Langen, R. Geiger, M. Kuhnert, B. Rauer, and J. Schmiedmayer, Nat. Phys. **9**, 640 (2013).
[11] C. Eigen, J. A. P. Glidden, R. Lopes, E. A. Cornell, R. P. Smith, and Z. Hadzibabic, Nature (London) **563**, 221 (2018).
[12] J. Berges, Sz. Borsányi, and C. Wetterich, Phys. Rev. Lett. **93**, 142002 (2004).
[13] A. Mitra, Annu. Rev. Condens. Matter Phys. **9**, 245 (2018).
[14] T. Langen, T. Gasenzer, and J. Schmiedmayer, J. Stat. Mech. (2016) 064009.
[15] T. Mori, T. N Ikeda, E. Kaminishi, and M. Ueda, J. Phys. B **51**, 112001 (2018).
[16] M. Marcuzzi, J. Marino, A. Gambassi, and A. Silva, Phys. Rev. Lett. **111**, 197203 (2013).
[17] B. Bertini, F. H. L. Essler, S. Groha, and N. J. Robinson, Phys. Rev. Lett. **115**, 180601 (2015).
[18] K. Mallayya, M. Rigol, and W. De Roeck, Phys. Rev. X **9**, 021027 (2019).
[19] P. Calabrese and J. Cardy, Phys. Rev. Lett. **96**, 136801 (2006).
[20] P. Calabrese and J. Cardy, J. Stat. Mech. (2007) P06008.
[21] M. Eckstein, M. Kollar, and P. Werner, Phys. Rev. Lett. **103**, 056403 (2009).
[22] B. Sciolla and G. Biroli, Phys. Rev. Lett. **105**, 220401 (2010).
[23] M. Schiró and M. Fabrizio, Phys. Rev. Lett. **105**, 076401 (2010).
[24] T. Kitagawa, A. Imambekov, J. Schmiedmayer, and E. Demler, New J. Phys. **13**, 073018 (2011).
[25] N. Tsuji and P. Werner, Phys. Rev. B **88**, 165115 (2013).
[26] N. Tsuji, M. Eckstein, and P. Werner, Phys. Rev. Lett. **110**, 136404 (2013).
[27] B. Sciolla and G. Biroli, Phys. Rev. B **88**, 201110(R) (2013).
[28] M. Heyl, A. Polkovnikov, and S. Kehrein, Phys. Rev. Lett. **110**, 135704 (2013).
[29] A. Chandran, A. Nanduri, S. S. Gubser, and S. L. Sondhi, Phys. Rev. B **88**, 024306 (2013).
[30] P. Smacchia, M. Knap, E. Demler, and A. Silva, Phys. Rev. B **91**, 205136 (2015).
[31] J. C. Halimeh, V. Zauner-Stauber, I. P. McCulloch, I. de Vega, U. Schollwöck, and M. Kastner, Phys. Rev. B **95**, 024302 (2017).

[32] J. C. Halimeh and V. Zauner-Stauber, Phys. Rev. B **96**, 134427 (2017).

[33] V. Zauner-Stauber and J. C. Halimeh, Phys. Rev. E **96**, 062118 (2017).

[34] J. C. Halimeh, M. Van Damme, V. Zauner-Stauber, and L. Vanderstraeten, Phys. Rev. Research **2**, 033111 (2020).

[35] I. Homrighausen, N. O. Abeling, V. Zauner-Stauber, and J. C. Halimeh, Phys. Rev. B **96**, 104436 (2017).

[36] J. Lang, B. Frank, and J. C. Halimeh, Phys. Rev. B **97**, 174401 (2018).

[37] J. Lang, B. Frank, and J. C. Halimeh, Phys. Rev. Lett. **121**, 130603 (2018).

[38] N. Defenu, T. Enss, and J. C. Halimeh, Phys. Rev. B **100**, 014434 (2019).

[39] T. Hashizume, I. P. McCulloch, and J. C. Halimeh, arXiv:1811.09275.

[40] T. Hashizume, J. C. Halimeh, and I. P. McCulloch, Phys. Rev. B **102**, 035115 (2020).

[41] B. Žunkovič, M. Heyl, M. Knap, and A. Silva, Phys. Rev. Lett. **120**, 130601 (2018).

[42] J. Zhang, G. Pagano, P. W. Hess, A. Kyprianidis, P. Becker, H. Kaplan, A. V. Gorshkov, Z.-X. Gong, and C. Monroe, Nature (London) **551**, 601 (2017).

[43] S. Smale, P. He, B. A. Olsen, K. G. Jackson, H. Sharum, S. Trotzky, J. Marino, A. M. Rey, and J. H. Thywissen, Sci. Adv. **5**, eaax1568 (2019).

[44] A. Chiocchetta, M. Tavora, A. Gambassi, and A. Mitra, Phys. Rev. B **91**, 220302(R) (2015).

[45] A. Maraga, A. Chiocchetta, A. Mitra, and A. Gambassi, Phys. Rev. E **92**, 042151 (2015).

[46] A. Chiocchetta, M. Tavora, A. Gambassi, and A. Mitra, Phys. Rev. B **94**, 134311 (2016).

[47] A. Chiocchetta, A. Gambassi, S. Diehl, and J. Marino, Phys. Rev. Lett. **118**, 135701 (2017).

[48] S.-K. Jian, S. Yin, and B. Swingle, Phys. Rev. Lett. **123**, 170606 (2019).

[49] H. K. Janssen, B. Schaub, and B. Schmittmann, Z. Phys. B **73**, 539 (1989).

[50] Z. B. Li, L. Schülke, and B. Zheng, Phys. Rev. Lett. **74**, 3396 (1995).

[51] S. Yin, P. Mai, and F. Zhong, Phys. Rev. B **89**, 144115 (2014).

[52] P. Gagel, P. P. Orth, and J. Schmalian, Phys. Rev. Lett. **113**, 220401 (2014).

[53] P. Gagel, P. P. Orth, and J. Schmalian, Phys. Rev. B **92**, 115121 (2015).

[54] K. G. Wilson and J. Kogut, Phys. Rep **12**, 75 (1974).

[55] D. S. Petrov, Phys. Rev. Lett. **115**, 155302 (2015).

[56] L. D. Landau and E. M. Lifshitz, *Statistical Physics* (Butterworth-Heinemann, 1999), Chap. 14.

[57] S. Coleman and E. Weinberg, Phys. Rev. D **7**, 1888 (1973).

[58] B. I. Halperin, T. C. Lubensky, and S.-K. Ma, Phys. Rev. Lett. **32**, 292 (1974).

[59] B. Ihrig, N. Zerf, P. Marquard, I. F. Herbut, and M. M. Scherer, Phys. Rev. B **100**, 134507 (2019).

[60] T. Senthil, A. Vishwanath, L. Balents, S. Sachdev, and M. P. A. Fisher, Science **303**, 1490 (2004).

[61] T. Senthil, L. Balents, S. Sachdev, A. Vishwanath, and M. P. A. Fisher, Phys. Rev. B **70**, 144407 (2004).

[62] A. W. Sandvik, Phys. Rev. Lett. **98**, 227202 (2007).

[63] F. S. Nogueira, S. Kragset, and A. Sudbø, Phys. Rev. B **76**, 220403(R) (2007).

[64] R. G. Melko and R. K. Kaul, Phys. Rev. Lett. **100**, 017203 (2008).

[65] M. S. Block, R. G. Melko, and R. K. Kaul, Phys. Rev. Lett. **111**, 137202 (2013).

[66] J. Lou, A. W. Sandvik, and N. Kawashima, Phys. Rev. B **80**, 180414(R) (2009).

[67] S. Pujari, K. Damle, and F. Alet, Phys. Rev. Lett. **111**, 087203 (2013).

[68] A. Nahum, J. T. Chalker, P. Serna, M. Ortuño, and A. M. Somoza, Phys. Rev. X **5**, 041048 (2015).

[69] F. Wang, S. A. Kivelson, and D.-H. Lee, Nat. Phys. **11**, 959 (2015).

[70] H. Shao, W. Guo, and A. W. Sandvik, Science **352**, 213 (2016).

[71] A. Nahum, P. Serna, J. T. Chalker, M. Ortuño, and A. M. Somoza, Phys. Rev. Lett. **115**, 267203 (2015).

[72] T. Sato, M. Hohenadler, and F. F. Assaad, Phys. Rev. Lett. **119**, 197203 (2017).

[73] G. J. Sreejith, S. Powell, and A. Nahum, Phys. Rev. Lett. **122**, 080601 (2019).

[74] Z.-X. Li, S.-K. Jian, and H. Yao, arXiv:1904.10975.

[75] Z.-X. Li, Y.-F. Jiang, S.-K. Jian, and H. Yao, Nat. Commun. **8**, 314 (2017).

[76] M. M. Scherer and I. F. Herbut, Phys. Rev. B **94**, 205136 (2016).

[77] L. Classen, I. F. Herbut, and M. M. Scherer, Phys. Rev. B **96**, 115132 (2017).

[78] S.-K. Jian and H. Yao, Phys. Rev. B **96**, 195162 (2017).

[79] S.-K. Jian and H. Yao, Phys. Rev. B **96**, 155112 (2017).

[80] E. Torres, L. Classen, I. F. Herbut, and M. M. Scherer, Phys. Rev. B **97**, 125137 (2018).

[81] B. Roy and V. Juričić, Phys. Rev. B **99**, 241103 (2019).

[82] S. Yin and Z. Y. Zuo, Phys. Rev. B **101**, 155136 (2020).

[83] A. F. Devonshire, Philos. Mag. **40**, 1040 (1949).

[84] From the field-theoretical effective model, Ω has two fixed points; one is zero, and the other is infinity [47]. The former represents the equilibrium limit, while the latter corresponds to the deep quench case. Here, we directly choose $\Omega \gg \Lambda$ (near the infinity fixed point), which represents the initial state being a completely disordered phase [44,46]. In this case, Ω can be set as a parameter rather than a scaling variable [44,46]. In real lattice model and experiments, the universal behaviors will not be changed as long as Ω is set outside the critical region. When Ω is set inside the critical region, the relaxation dynamics is affected by the equilibrium critical point in the early stage and then crosses over to the stage controlled by the dynamical critical point since Ω is relevant [47].

[85] A. Mitra and T. Giamarchi, Phys. Rev. Lett. **107**, 150602 (2011).

[86] A. Mitra, Phys. Rev. Lett. **109**, 260601 (2012).

[87] In principle, g_q always equals g_c in the UV limit. Here, to emphasize the special role played by g_q, we just formally assume that g_q in the UV scale is zero, while g_c remains nonzero.

[88] M. A. Stephanov, Phys. Rev. D **52**, 3746 (1995).

[89] S. Hesselmann and S. Wessel, Phys. Rev. B **93**, 155157 (2016).

[90] K. R. Fratus and M. Srednicki, Phys. Rev. E **92**, 040103(R) (2015).

[91] Y. Kato and T. Misawa, Phys. Rev. B **92**, 174419 (2015).

[92] A. B. Harris, T. C. Lubensky, and E. J. Mele, Phys. Rev. B **40**, 2631(R) (1989).
[93] A. H. Castro Neto, F. Guinea, N. M. R. Peres, K. S. Novoselov, and A. K. Geim, Rev. Mod. Phys. **81**, 109 (2009).
[94] D. Greif, G. Jotzu, M. Messer, R. Desbuquois, and T. Esslinger, Phys. Rev. Lett. **115**, 260401 (2015).
[95] C. Gross and I. Bloch, Science **357**, 995 (2017).
[96] T. Kinoshita, T. Wenger, and D. S. Weiss, Nature (London) **440**, 900 (2006).
[97] S. Hofferberth, I. Lesanovsky, B. Fischer, T. Schumm, and J. Schmiedmayer, Nature (London) **449**, 324 (2007).
[98] S. Erne, R. Bücker, T. Gasenzer, J. Berges, and J. Schmiedmayer, Nature (London) **563**, 225 (2018).
[99] M. Prüfer, P. Kunkel, H. Strobel, S. Lannig, D. Linnemann, C. Schmied, J. Berges, T. Gasenzer, and M. K. Oberthaler, Nature (London) **563**, 217 (2018).
[100] E. Nicklas, M. Karl, M. Höfer, A. Johnson, W. Muessel, H. Strobel, J. Tomkovič, T. Gasenzer, and M. K. Oberthaler, Phys. Rev. Lett. **115**, 245301 (2015).
[101] R. Boyack, H. Yerzhakov, and J. Maciejko, arXiv:2004.09414.
[102] P. Jakubczyk, Phys. Rev. B **79**, 125115 (2009).
[103] P. Jakubczyk, W. Metzner, and H. Yamase, Phys. Rev. Lett. **103**, 220602 (2009).